Peeling off an elastica from a smooth attractive substrate

Xabier Oyharcabal* and Thomas Frisch†

Institut de Recherche sur les Phénomènes Hors Équilibre, UMR 6594, CNRS, Université d'Aix-Marseille, Marseille, France

(Received 27 September 2004; published 17 March 2005)

Using continuum mechanics, we study theoretically the unbinding of an inextensible rod with free ends attracted by a smooth substrate and submitted to a vertical force. We use the elastica model in a medium-range van der Waals potential. We numerically solve a nonlinear boundary value problem and obtain the force-stretching relation at zero temperature. We obtain the critical force for which the rod unbinds from the substrate as a function of three dimensionless parameters, and we find two different regimes of adhesion. We study analytically the contact potential case as the van der Waals radius goes to zero.

DOI: 10.1103/PhysRevE.71.036611 PACS number(s): 46.25.Cc, 68.35.Np

Adhesion and elasticity play an important role in biophysics and in materials science from both the fundamental and applied points of view [1]. The nanomanipulation of single stiff polymer chains and single semiflexible biological macromolecules can give insight into the mechanical properties of macromolecules such as DNA or Actin. Forces on the scale of piconewtons have been measured with imposed deformation on the scale of the nanometer with atomic force microscopes (AFM's) [2] or optical tweezers [3]. Using these experimental techniques the different mechanisms of adsorption between a macromolecule and a substrate can be investigated. On a larger scale and from a further perspective, the process of dry adhesion between a lizard such as the gecko and a rough substrate involves a mechanism supported by the van der Waals molecular forces [4]. A better understanding of this mechanism could lead to the creation of new type of adhesives [5] or better design of nanorobotics adhesive machines. The physics behind the breaking of adhesive junctions involves many different molecular processes which depend on the surface characteristics and on the nature of the intermolecular forces. It is therefore relevant to examine simple models in which elasticity and intermolecular forces (adhesion) play an interconnected role [6–13]. In this article, we examine the simple case of a free semiflexible rod described by its bending energy, in adhesion with a smooth nonpolar substrate. The rod with free ends is attracted by the surface by a van der Waals–like force while a vertical stretching force is applied at one of its ends. Using Euler's elastica model [14], we study the force stretching relation of the ground state (zero temperature) of the inextensible rod. We numerically measure the vertical deflection of the tip of the rod on which the vertical force is applied. We obtain, as a function of three dimensionless parameters, the force-stretching relation and the critical force at which unbinding takes place, by solving numerically a boundary value problem. We find two different regimes for the critical force for low and high adhesion energy. Finally, we study the limiting case of the contact potential by taking the limit of zero van der Waals radius and we recover an analytical solution.

*Electronic address: oyharcabal@irphe.univ-mrs.fr

†Electronic address: frisch@irphe.univ-mrs.fr

We consider an inextensible rod described by two parameters: κ, the bending coefficient, and L, its length. The attracting potential is described by two parameters: W, the adhesion constant, and σ, the van der Waals radius. As shown in Fig. 1, we apply at one end of the rod a vertical force F. We focus here on the case of a rod of very small diameter d such that $d < \sigma$. In contrary to the Hertz contact problem [14], the cross section of the rod does not deform. Here, we assume that the local radius of curvature of the rod is much larger than its diameter d. This enables us to make use of the elastica model. We assume that the interaction between the rod and the semi-infinite nonpolar substrate can be modeled by a medium-range van der Waals-like potential [1]. This potential combines a hard-core repulsive term and a medium-range attractive term:

$$V(y) = W\left[\left(\frac{\sigma}{y}\right)^9 - \left(\frac{\sigma}{y}\right)^3\right]. \tag{1}$$

Here W is the adhesion energy per unit length and σ the van der Waals radius. In this article, we shall neglect the effect of thermal fluctuations. This is justified when the transverse fluctuations of the rod L^2/L_p are small compared to its length L so that $L < L_p = \kappa/k_bT$ where L_p is the persistence length [15]. Furthermore, we suppose that the adhesion energy is

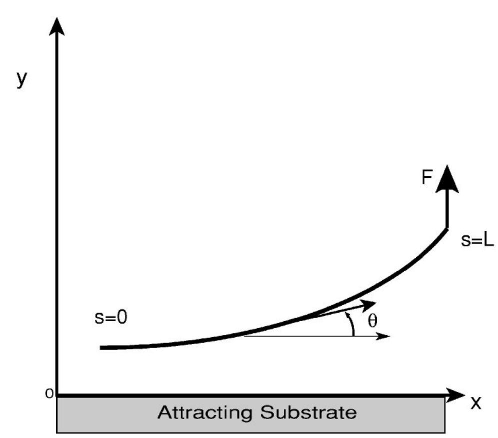

FIG. 1. Sketch of the rod attracted by the substrate and submitted to a vertical force.

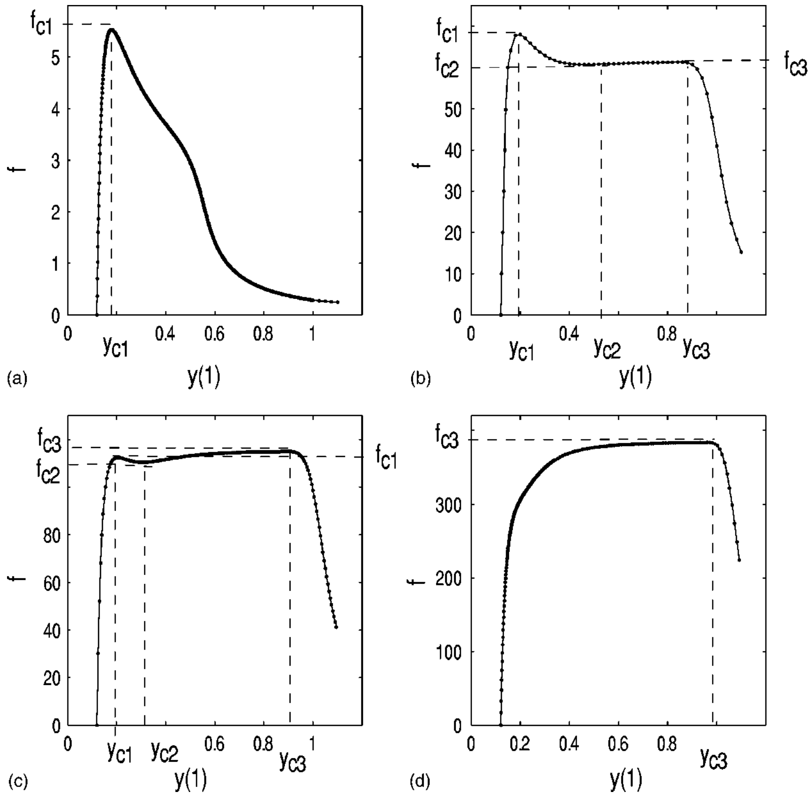

FIG. 2. Force-stretching plot for four values of w showing the diversity of solutions for $\epsilon = 0.1$. (a) $w=6$, (b) $w=160$, (c) $w=300$, and (d) $w=1000$ obtained by numerical solutions of Eqs. (4). f is the intensity of the force applied at the end of the rod, and $y(1)$ is the vertical height of the end of the rod measured from the substrate.

large so that $W > k_b T/\sigma$. This ensures that the rod is in strong adhesion with the substrate. The total energy of the system is, then,

$$E = \frac{\kappa}{2}\int_0^L \dot{\theta}^2 ds + \int_0^L V(y)ds - Fy(L), \tag{2}$$

where the first term is the bending energy of the rod, the second term is the interaction with the substrate, and the third term is the work of the applied force. Here s is the arclength along the rod, the dot is the derivative with respect to the arclength, θ is the angle between the tangent to the rod and the x axis, and F is the intensity of the vertical force that is applied at $s=L$ (Fig. 1). The full shape of the rod can be reconstructed in the Cartesian frame of coordinates by the use of the geometrical relations $\partial y = \sin\theta\,\partial s$ and $\partial x = \cos\theta\,\partial s$. We choose a set of dimensionless length and energy in the following way: $\overline{s}=s/L$, $\overline{x}=x/L$, $\overline{y}=y/L$, $\overline{E}=EL/\kappa$. The Lagrange multiplier $\gamma(s)$ has to be introduced because y and θ are mutually dependent [16]. After dropping the overbars on the dimensionless variables, we obtain

$$E = \frac{1}{2}\int_0^1 \dot{\theta}^2 ds + w\int_0^1 \left[\left(\frac{\epsilon}{y}\right)^9 - \left(\frac{\epsilon}{y}\right)^3\right]ds + \int_0^1 \gamma(s)[\dot{y} - \sin\theta]ds - fy(1). \tag{3}$$

Here $w=WL^2/\kappa$, $\epsilon=\sigma/L$, and $f=FL^2/\kappa$ are the three dimensionless parameters of the system. The boundary conditions at the free ends of the rod are $\dot{\theta}(0)=0$ and $\dot{\theta}(1)=0$ since both ends of the rod are torque free. The minimization of the energy E leads to the following system of nonlinear ordinary equations:

$$\ddot{\theta} + \gamma\cos\theta = 0, \quad \dot{\gamma} = \frac{\partial v}{\partial y}, \quad \dot{y} = \sin\theta. \tag{4}$$

Here $v(y)=w[(\epsilon/y)^9-(\epsilon/y)^3]$. The boundary conditions are $\dot{\theta}(0)=0$, $\gamma(0)=0$, $\dot{\theta}(1)=0$, and $\gamma(1)=f$. The unknown conditions are $\theta(0)$ and $y(0)$. Equations (4) are solved efficiently by a standard shooting method. In the absence of the stretching force ($f=0$), the only stable solution is $y=y_0=3^{1/6}\epsilon$ which corresponds to the minimum of the adhesion potential. We then use a classical continuation method [17] in order to follow accurately the branch of solutions of Eqs. (4). We first focus our attention on the dependence of the height $y(1)$ on the force intensity f. Figure 2 shows the force-stretching plot [f versus $y(1)$] for four values of w at $\epsilon=0.1$. Figure 2(a) shows the force-stretching curve for $w=6$. It has a maximum for $f=f_{c1}$ and $y=y_{c1}$. The critical force f_{c1} is the unbinding force, and it corresponds to the maximum force that can be applied to the rod without which it unbinds and y_{c1} is the critical height marking the border between two regions of different behavior. For $y(1)\in[y_0, y_{c1}]$ the system has a springlike behavior and the force increases with displacement, whereas for higher values of $y(1)$ it behaves like an antispring and the force decreases with displacement. It is important to note that the antispring branches are mechanically stable if the height is fixed. Figures 2(b) and 2(c) correspond to the typical behavior for intermediate values of w. A second maximum appears for $f=f_{c3}$ and $y=y_{c3}$ and of course a minimum $f=f_{c2}$ and $y=y_{c2}$. In this regime four regions appear, passing alternatively from a springlike behav-

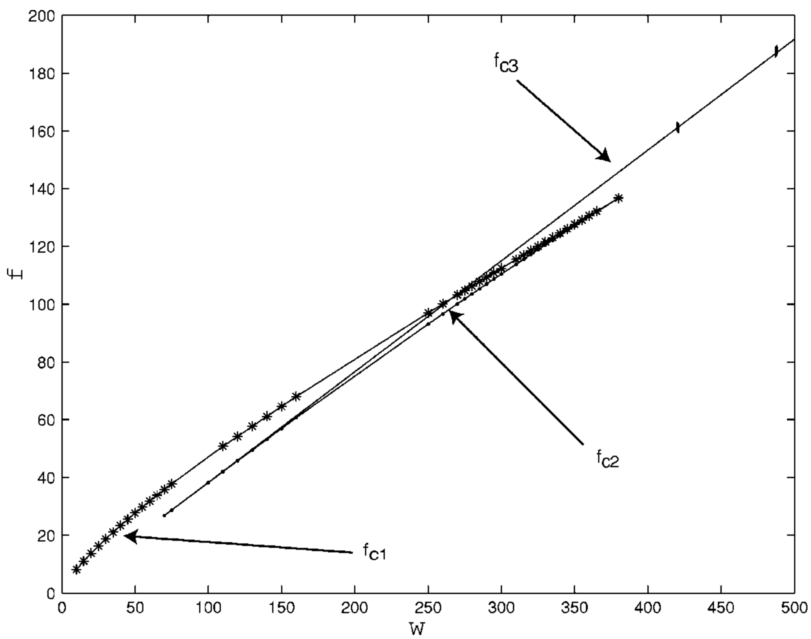

FIG. 3. State diagram for $\epsilon=0.1$ in the nondimensional (f,w) parameter space. The values of the critical force are obtained by analyzing every force-stretching plot obtained by numerical resolution of Eqs. (4).

ior to an antispringlike behavior. The critical force corresponding to the unbinding force is now $\max(f_{c1},f_{c3})$. In Fig. 2(d), which is representative of the high values of w, the maximum (f_{c1},y_{c1}) disappears and consequently the unbinding force is f_{c3}. In order to evaluate the role of each parameter, we made a quantitative phase diagram (f,w) of the system as shown in Fig. 3. We also present a qualitative sketch of it on Fig. 4 for more clarity. The phase diagram shows three different regions for this system. The upper region (A) of Fig. 4 is the unbounded region. In the region (C), for each value of f there are one or two values of $y(1)$ corresponding to one or two shapes of the rod. In the grey region (B), there are four possible shapes of the rod for each value of the force f. As expected, there is a maximum value of $y(1)$ near $1+y_0$ for which the solutions disappear as a consequence of the inextensibility of the rod [18]. We now focus on the

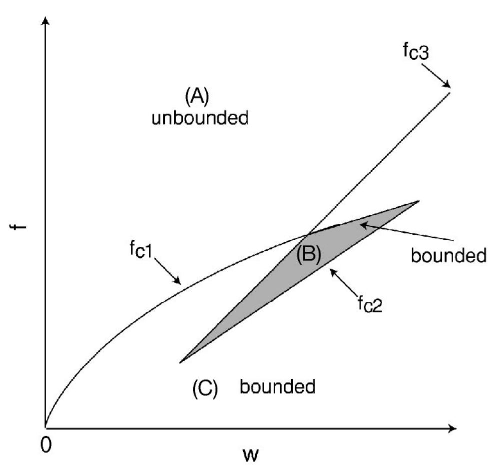

FIG. 4. Sketch of the state diagram for $\epsilon=0.1$ in the force-adhesion (f,w) parameter space. The upper region (A) is the unbounded region in which there are no solution of Eqs. (4). The (B) and (C) regions are the bounded regions. In the (B) region there are four solutions, and in the (C) region there are at most two solutions.

dependence of the unbinding force versus ϵ. Figure 5 shows the force-stretching curves for different values of ϵ obtained by numerical resolution of Eqs. (4). In the limit $\epsilon\rightarrow 0$, the numerical calculation of the solutions of Eqs. (4) becomes stiff. As we decrease the value of ϵ, we find that the critical force increases very rapidly as shown in Fig. 5. A log-log plot of f_c versus ϵ on four decades reveals that f_c diverges like $\epsilon^{-1/2}$. Furthermore, as shown in Fig. 3, $f_{c1}\sim w^{3/4}$ for small w. This result is verified for $\epsilon=0.1$ and $\epsilon=0.01$ (data not shown here). Using our numerical results we find that the global scaling behavior for small w is $f_c\sim w^{3/4}/\epsilon^{1/2}$. If we express these scaling relations using the dimensional parameters, we obtain $F_c\sim W^{3/4}\kappa^{1/4}/\sigma^{1/2}$, whereas for high w, $f_c\sim w$ so that $F_c\sim W$. Let us choose some values for the physical parameters of a nanorod. A typical distance range for the van der Waals forces is $\sigma\sim 1$ nm and $R\sim 1$ nm (R is the radius of the rod). For the adhesion force $W\sim aR$, here $a\sim 0.01$ J m^{-2} is a typical adhesion energy due to the van der Waals forces. The rigidity of the rod, κ, is directly related to its Young modulus Y through $\kappa\sim YR^4$. For $Y=10^{10}$ Pa, corresponding to the Young modulus of a hair, we have $\kappa=10^{-26}$ J m. Thus, for a nanorod of length $L\sim 10^{-8}$ m, a typical critical force will be of the order of the $F_c\sim W^{3/4}\kappa^{1/4}/\sigma^{1/2}\sim 10^{-10}$ N. We will now consider the contact potential case for which we shall provide an analytical solution. There is now a discontinuity in the adhesion potential at $y=0$. We can divide the rod in two segments. The first one is straight and lies on the substrate. This segment does not have curvature and contributes to the total energy through the adhesion energy. The second segment is not in contact with the substrate and has only bending energy. Thus, the energy functional can be written as

$$E=\frac{1}{2}\int_{s_0}^{1}\dot{\theta}^2 ds - ws_0 - fy(1), \tag{5}$$

where s_0 is the length of the rod which is in contact with the substrate. Following [16], the first variation of the energy

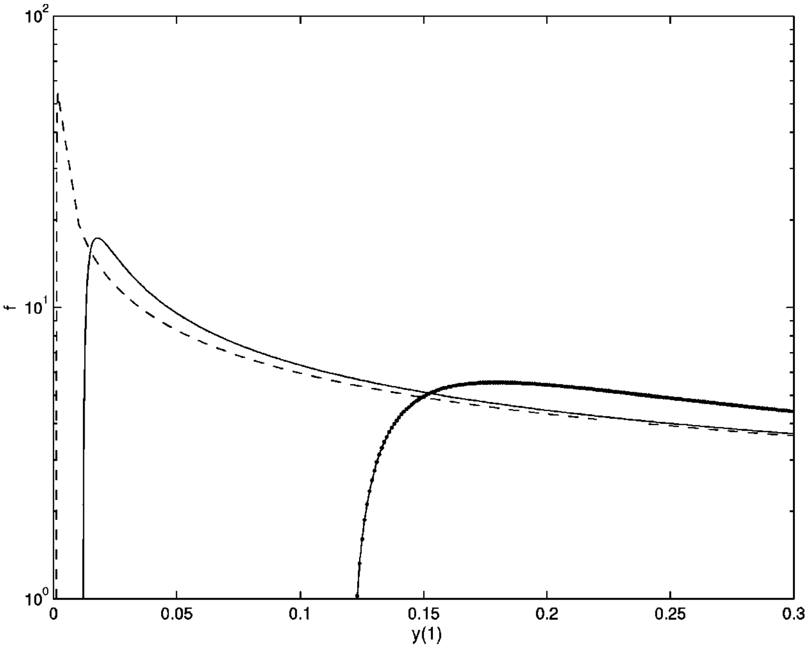

FIG. 5. Numerical solutions of Eqs. (4). Force-stretching plot of f versus $y(1)$ for $w=6$: dashed line $\epsilon=0.001$, solid line $\epsilon=0.01$, and thick solid line $\epsilon=0.1$.

functional leads to a system of two equations:

$$\ddot{\theta} = -f\cos(\theta), \quad \dot{y} = \sin\theta. \tag{6}$$

The boundary conditions are $\theta(s_0)=0$ and $\dot{\theta}(s_0)=\sqrt{2w}$ as shown by [6,16]. Solving these equations leads to the following relation for s_0:

$$s_0 = 1 - \int_0^{\theta(1)} \frac{\partial\theta}{\sqrt{2[w - f\sin(\theta)]}}, \tag{7}$$

where $\sin\theta(1)=w/f$. The shape of the rod is given implicity by

$$\int_{\theta(s)}^{\theta(1)} \frac{\partial\theta}{\sqrt{2[w - f\sin(\theta)]}} = 1 - s, \tag{8}$$

for $s > s_0$ and $\theta(s)=0$ when $0 < s < s_0$. We can now obtain the full shape of the rod, the contact length s_0, and the force-stretching relation by solving Eqs. (7) and (8). As shown in Fig. 6, the force-stretching plot is monotonically decreasing and the rod has an antispring behavior. In this case, the force is infinite when $y(1)$ goes to zero since we are in presence of a contact potential. Such a result is consistent with the limit of ϵ going to zero of the van der Waals model; see Fig. 5. As a consequence of the antispring behavior, as we decrease the force, the contact length s_0 diminishes until a critical force

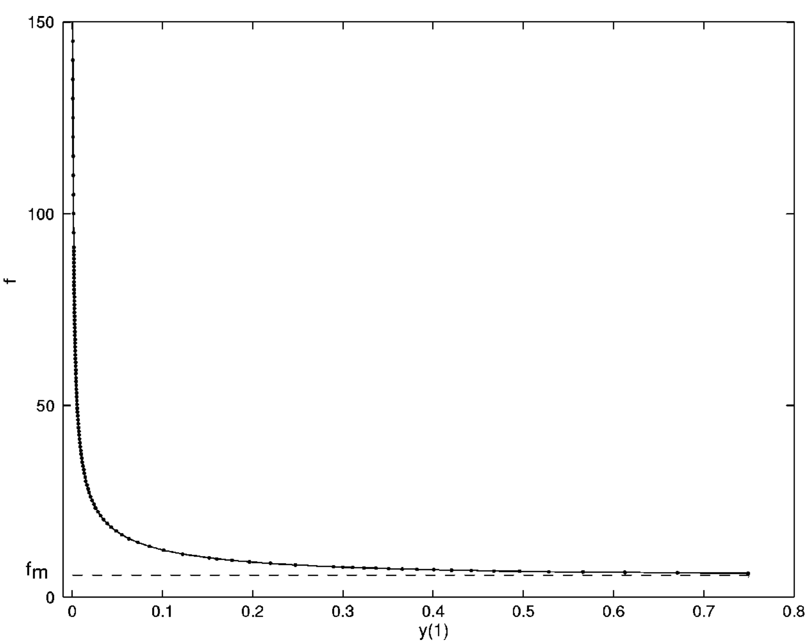

FIG. 6. Theoretical force-stretching plot for $w=6$ in the case of the contact potential obtained by solving Eqs. (7) and (8). The force is infinite for $y(1)=0$ and f_m is a lower limit.

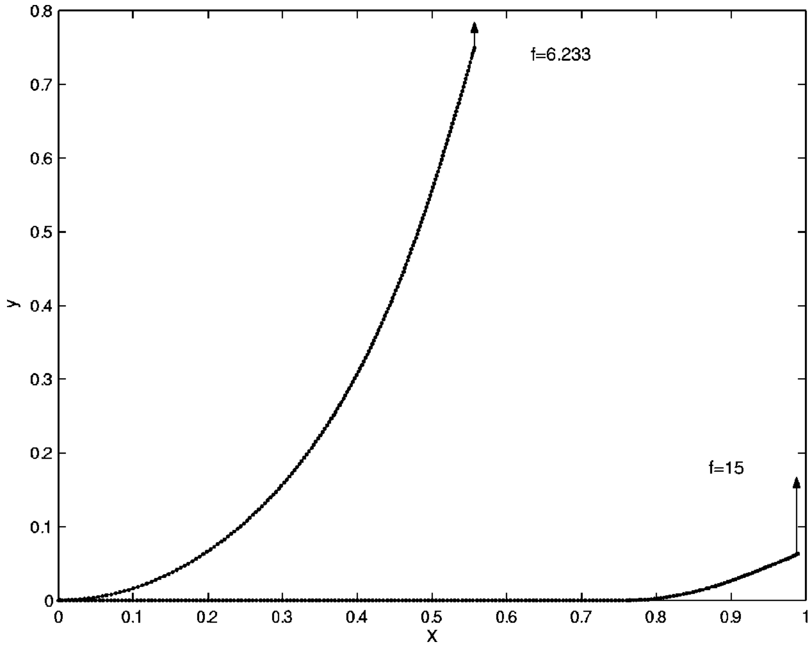

FIG. 7. Shape of the rod under stretching for two values of f for the contact potential obtained by solving Eqs. (7) and (8). Top: $f=f_m=6.233$. Bottom: $f=15$.

$f_m(w)$ is reached. This critical force f_m, for which $s_0=0$, is a solution of the following equation:

$$\int_0^{\theta(1)} \frac{\partial\theta}{\sqrt{2[w-f_m\sin(\theta)]}} = 1. \qquad (9)$$

Figure 7 shows two shapes of the rod corresponding to two different values of the applied force. These plots are obtained by the integration of $\theta(s)$. The bottom plot of Fig. 7 corresponds to $f=15$, in this case $s_0>0$, while the top plot corresponds to $f=f_m$.

To summarize, we have studied the ground state of a semiflexible rod at zero temperature in a smooth adsorbing potential as a function of three dimensionless parameters. We have solved the boundary value problem using a shooting method, and we have found very different behaviors. Depending on the values of the parameters, the rod can have mostly a springlike behavior or an antispring behavior. We also have shown that the unbinding force scales like $F_c \sim W$ for high W and $F_c \sim W^{3/4}\kappa^{1/4}/\sigma^{1/2}$ for low W. We have compared the above results to those in the limit of $\epsilon=0$, and we recover the solution of the contact potential in the limit of ϵ going to zero. We hope that this work will motivate more experimental work on the force-stretching measurements of adhering macromolecules. It would be interesting to study the limit $d \gg \sigma$, which is more accessible experimentally (d is the diameter of the rod), but in this case the rod model would have to be changed and the Hertz contact theory with adhesion should be included [7]. Our study does not take into account the effect of the finite radius of the rod; complex elastic deformations are expected around the contact point s_0. Molecular dynamics simulations are in progress for a study of the region around the contact point s_0. Moreover, we suggest that it could be possible to study experimentally, using an atomic force microscope or optical magnetic tweezers, the detachment of a semi-flexible biopolymer (DNA or Actin) strongly adsorbed on a substrate.

We would like to thank Simona Bodea, Alberto Verga, Marc Georgelin, Moktar Adda-Bedia, and Yves Pomeau, for stimulating discussions.

[1] J. N. Israelachvili, *Intermolecular and Surface Forces* (Academic, New York, 1992).
[2] M. Rief, H. Clausen-Schauman, and H. Gaub, Nat. Struct. Biol. **6**, 346 (1999).
[3] D. E. Smith, S. Tans, S. Smith, S. Grimes, D. L. Anderson, and C. Bustamante, Nature (London) **413**, 748 (2001).
[4] K. Autumn, M. Sitti, Y. Liang, A. Peattie, W. Hansen, S. Sponberg, T. Denny, R. Fearing, J. Israelachvili, and R. Full, Proc. Natl. Acad. Sci. U.S.A. **99**, 12 252 (2002).
[5] A. K. Geim, S. V. Dubonos, I. V. Grigorieva, K. S. Novoselov, A. A. Zhudov, and S. Y. Shapoval, Nat. Mater. **2**, 161 (2003).
[6] J. Obreimoff, Proc. R. Soc. London, Ser. A **127**, 290 (1930).
[7] K. L. Johnson, K. Kendall, and A. D. Roberts, Proc. R. Soc. London, Ser. A **324**, 301 (1971).
[8] D. Maugis, J. Colloid Interface Sci. **150**, 243 (1992).
[9] P. Attard and J. L. Parker, Phys. Rev. A **46**, 7959 (1992).
[10] P. Attard, Phys. Rev. E **63**, 011601 (2000).
[11] A. Ghatak, M. K. Chaudhury, V. Shenoy, and A. Sharma, Phys. Rev. Lett. **85**, 4329 (2000).
[12] R. H. Plaut, A. J. Dalrymple, and D. A. Dillard, J. Adhes. Sci. Technol. **15**, 565 (2001).
[13] J. Bico, B. Roman, L. Moulin, and A. Boudaoud, Nature (London) **432**, 690 (2004).
[14] L. Landau and E. M. Lifshitz, *Theory of Elasticity* (Pergamon,

New York, 1959).
[15] L. Landau and E. M. Lifshitz, *Statistical Physics* (Butterworths-Heinemann, London, 1980).
[16] U. Seifert, Phys. Rev. A **43**, 6803 (1991).
[17] L. Mahadevan and J. Keller, Proc. R. Soc. London, Ser. A **452**, 1679 (1996).
[18] In this work, we do not focus on the maximal height of the end of the rod $y(1)$ but on the critical forces.